Precision Agriculture (2025) 26:28
https://doi.org/10.1007/s11119-025-10228-2

Forecasting field rice grain moisture content using Sentinel-2 and weather data

James Brinkhoff[1] · Brian W. Dunn[2] · Tina Dunn[2] · Alex Schultz[2] · Josh Hart[2]

Accepted: 25 January 2025

Abstract
Optimizing the timing of rice paddy drainage and harvest is crucial for maximizing yield and quality. These decisions are guided by rice grain moisture content (GMC), which is typically determined by destructive plant samples taken at point locations. Providing rice farmers with predictions of GMC will reduce the time burden of gathering, threshing and testing samples. Additionally, it will reduce errors due to samples being taken from unrepresentative areas of fields, and will facilitate advanced planning of end-of-season drain and harvest timing. This work demonstrates consistent relationships between rice GMC and indices derived from Sentinel-2 satellite imagery, particularly those involving selected shortwave infrared and red edge bands (r=0.84, 1620 field samples, 3 years). A methodology was developed to allow forecasts of grain moisture past the latest image date to be provided, by fusing remote sensing and accumulated weather data as inputs to machine learning models. The moisture content predictions had root mean squared error between 1.6 and 2.6% and R^2 of 0.7 with forecast horizons from 0 to 28 days. Time-series grain moisture dry-down predictions were summarized per field to find the optimal harvest date (22% grain moisture), with an average RMSE around 6.5 days. The developed methodology was operationalized to provide rice growers with current and projected grain moisture, enabling data-driven decisions, ultimately enhancing operational efficiency and crop outcomes.

Keywords Rice · Grain moisture · Harvest timing · Machine learning · Remote sensing · Crop maturity

✉ James Brinkhoff
james.brinkhoff@une.edu.au

[1] Applied Agricultural Remote Sensing Centre, University of New England, Armidale 2351, New South Wales, Australia

[2] Soil and Water, Department of Primary Industries and Regional Development, Yanco 2703, New South Wales, Australia

Published online: 31 January 2025

Introduction

Precision agriculture technologies aim to improve productivity and environmental outcomes by optimizing field management. While spatial aspects of field management practices, such as soil improvement, seed and nutrient distribution and yield mapping have been a key focus (Nowak, 2021), the timing of crop management operations is equally critical. In rice, the timing of sowing (Brinkhoff et al., 2023), fertilizer applications (Peng & Cassman, 1998; Dunn et al., 2014), water application (Dunn & Gaydon, 2011; Humphreys et al., 2006), field drainage and harvest (McCauley & Way, 2002; Counce et al., 1990) all significantly impact yield, quality, water use and emissions.

Determining the optimal time to cease irrigation or drain fields is a critical end-of-season decision for irrigated rice growers. This decision must balance the need to ensure that the grains have reached maximum dry matter accumulation (physiological maturity) (Dingkuhn & Le Gal, 1996), with the need to avoid delays in harvest. Harvest timing is pivotal (Wang et al., 2021), as harvesting too early can result in grains with high moisture content that require additional drying and can incur processor penalties, while harvesting too late can lead to dry grains that are susceptible to fissuring (Siebenmorgen et al., 2007) particularly if there is rain during the dry-down period (R. Lu et al., 1995). This can cause a reduction in the proportion of unbroken grains after milling (head rice yield) (Calderwood et al., 1980), which can lead to reduced profit. In Australia, harvest is recommended when rice has reached 22% moisture (Ward et al., 2021), and similar values have been found to result in optimal head rice yield in the US mid-south (Siebenmorgen et al., 2007).

For the broader industry, accurate forecasts of grain moisture content (GMC) across many fields are valuable to plan harvest operations, manage grain storage and transport logistics. Integrating harvest timing prediction with yield forecasts (Brinkhoff et al., 2024) adds further value to rice processors in managing and marketing grain. An additional benefit at the industry scale is enabling powerful analytics of the drivers of grain quality (Clarke et al., 2024), so that accurate extension messages can be delivered to farmers with the goal of improving outcomes in future seasons.

Despite the importance of estimating GMC in guiding drainage and harvest decisions, common practice often relies on point measurements such as the “squeeze-test”, moisture meters or more recent instruments (Flor et al., 2022; Yang et al., 2021), which are not scalable and fail to capture spatial variability across large fields. Spatial variability of rice maturity can be caused by factors such as variations in water temperature (Sharifi et al., 2018), phenology, soil type, and nitrogen uptake (Brinkhoff et al., 2023). This variability renders point samples unreliable for estimating the field average GMC or the spatial variability of GMC, particularly in the context of multi-hectare mechanized fields.

To address these challenges, researchers have sought to provide more scalable and spatial estimates of GMC in grain crops. For instance, optimum harvest timing for soy bean and maize has been estimated using weather data and Henderson-Perry dry-down equations (Martinez-Feria et al., 2019; Chazarreta et al., 2023), though they relied on in-field measurements of moisture at physiological maturity to determine initial conditions. Other work used data-driven models with inputs including days since sowing and weather to predict GMC (Abdollahpour et al., 2020). However, weather and sowing timing may not provide enough information to accurately predict GMC, as factors such as variety and nitrogen status also have an effect (Brinkhoff et al., 2023).

Remote sensing is a promising tool to estimate GMC across many large fields. Strong correlations between ratios of reflectances and panicle dry biomass have been demonstrated Peng et al. (2024), noting that remote sensing doesn't observe the panicles themselves but rather senses pigments that are related to grain ripening. Other studies have shown relationships between GMC and the normalized difference vegetation index (Dunn & Dunn, 2021), between GMC and remotely sensed canopy chlorophyll content (Xu et al., 2019), and have developed machine learning models to predict GMC from multispectral and hyperspectral imagery (Wu et al., 2024). However, many of these studies are limited by using data from a single season and small study area, raising questions about generalizability to new seasons and sites (Filippi et al., 2025). Recently, Yang et al. (2025) proposed using multispectral imagery collected using unmanned aerial vehicles to predict GMC, achieving low errors in a small area. However, as they noted, there is a need to use satellite imagery for broad-scale application, and to include weather data to enable forecasting GMC beyond the image collection date.

This work aims to develop predictive models for rice GMC using Sentinel-2 satellite data and weather data, using three years of field GMC samples collected from many commercial rice crops spread across the primary growing region in Australia. First, the relationship between rice GMC and co-incident imagery was investigated. Then machine learning models were trained, integrating input features from satellite imagery and accumulated weather variables, allowing projection of GMC beyond each image date by integrating weather forecasts. The model performance was assessed in terms of both GMC prediction accuracy, and the accuracy of predicted optimum harvest date (where GMC=22%).

Methods

Field data

There were a total of 247 sites over the three years, which are shown on the map in Fig. 1. There were two types of sites. The first type were point locations in larger commercial rice fields. These had the location marked with a pole and the coordinates were recorded using a GPS system. The second type of sites were large experiment plots with a range of nitrogen rates, also located in commercial fields. There were 3–9 plots in each experiment, and each plot is referred to as a site. Nitrogen affects flowering and dry-down (Brinkhoff et al., 2023), so these plots were included with the aim of generating data to allow the GMC models to learn these effects. The plots were large enough (greater than 30 m per side) to ensure they enclosed at least one Sentinel-2 pixel. The GMC samples were collected from the middle of each plot. The plots were clearly visible in the imagery, so the sample locations were refined using image inspection.

Each site was sampled on multiple dates (see Table 1), targeting GMC values from 30 to 18%. There were on average 6–7 samples per site with 4–6 days between samples. The 7 rice varieties (and number of samples per variety) were Koshihikari (7), Opus (7), Langi (10), Viand (101), Sherpa (121), Reiziq (150) and V071 (1213). V071 was the dominant variety grown in the area, hence the larger number of samples for this variety.

Grain moisture content (GMC %) was determined for each sample using the following method. Samples were collected after morning dew had evaporated. Three hand grabs

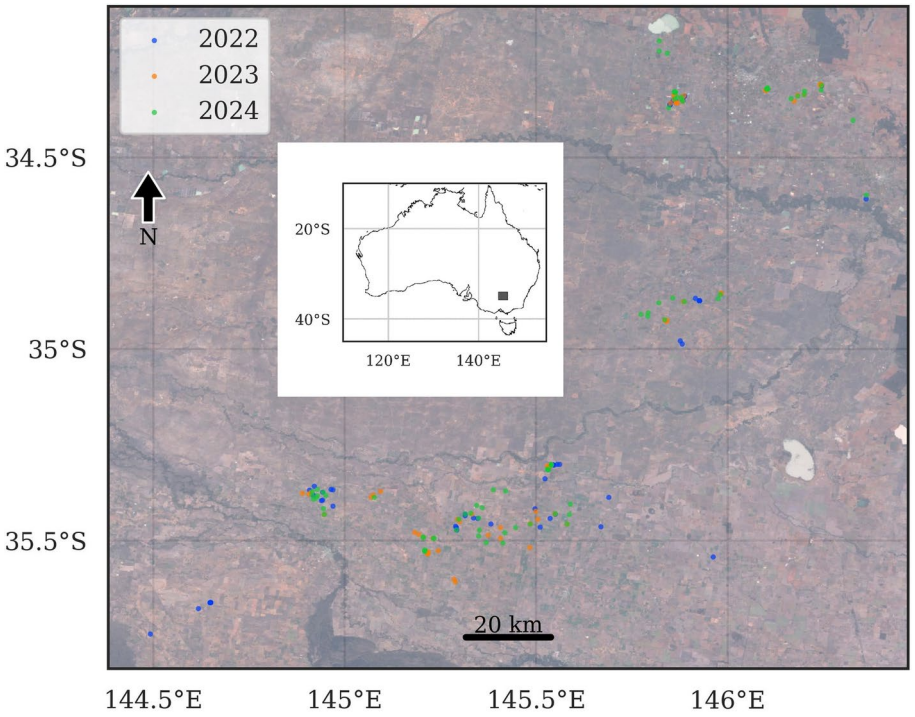

Fig. 1 Map of sites where rice grain moisture content was sampled each year (total of 247 sites); the inset shows the study area in relation to Australia

Table 1 Number of sites and samples for each year

Year	Sites	Number of samples	Average samples per site	Average days between samples
2022	75	451	6	6
2023	77	536	7	5
2024	95	622	7	4

were cut and bagged. These were then threshed, obtaining approximately 500 g of grain. The moisture content of the samples were determined on the same day using near-infrared transmission instruments, the Cropscan 2000B (Next Instruments, Condell Park, Australia). These instruments had previously been calibrated using 197 rice samples that had their moisture content determined using the two-stage air-oven reference method (AACC, 1999), with GMC ranging from 12 to 30%. The calibration was tested on independent samples with an R^2 of 0.97.

Remote sensing data

For each site, a time-series of Sentinel-2 data was generated using Google Earth Engine (Gorelick et al., 2017), by computing the pixel reflectance value at each site's point location. The reflectances in the ten bands with 10–20 m resolution were extracted, as listed in Table 2. This process was performed using both top of atmosphere (TOA, L1C) and surface

Table 2 Variables used in grain moisture prediction models

Feature set name	Name	Details
Rice variety	Variety	Categorical [Reiziq, V071, Langi, Sherpa...]
Sentinel-2 reflectances	B	Blue (490nm, 10m)
	G	Green (560nm, 10m)
	R	Red (665nm, 10m)
	RE1	Red edge (705nm, 20m)
	RE2	Red edge (740nm, 20m)
	RE3	Red edge (780nm, 20m)
	NIR1	Near infrared (835nm, 10m)
	NIR2	Near infrared (865nm, 20m)
	SWIR1	Shortwave infrared (1610nm, 20m)
	SWIR2	Shortwave infrared (2200nm, 20m)
Weather	Days	Number of accumulated days
	Tmin	Minimum daily temperature (^{0}C)
	Tmax	Maximum daily temperature (^{0}C)
	Srad	Solar radiation (MJ/m^2)
	RH(Tmax)	Relative humidity at time of Tmax (%)
	RH(Tmin)	Relative humidity at time of Tmin (%)
	ET	Short crop reference evapotranspiration (mm)
	DD	Degree days, base 10 (^{0}C)
	Rain	Daily rainfall (mm)
Combinations	All ND	All 45 independent normalized difference spectral indices ND(b1,b2), where b1,b2 are the reflectances listed above
	All weather	All weather parameters listed above
	Temps	Tmin and Tmax

reflectance (SR, L2A) data in order to compare the accuracy of GMC models built using these different processing levels.

The Cloud Score + product (Pasquarella et al., 2023) was used to mask cloud and cloud shadow. This product is based on a regression model, trained using a video analysis approach, and provides a continuous cloud score for each pixel. Pixels with a cloud score below 0.7 were masked.

After removing data affected by cloud, the time-series in each of the reflectance bands for each sample site was interpolated to a daily basis and smoothed using a Whittaker smoother (Eilers, 2003). This algorithm has advantages over the commonly used Savitzky-Golay filter, including smoother behavior at the end points of data, which is important for real-time applications (Schmid et al., 2022). The smoothing parameter λ was set to 500, which provided a good balance between removing noise, while retaining the real detail of the crop time-series.

Rather than limiting the models to use a small number of indices based on pre-conceived assumptions, the normalized difference spectral indices (NDSIs) based on all independent combinations of reflectances were derived:

$$ND(b1, b2) = (b1 - b2)/(b1 + b2) \quad (1)$$

For example, ND(NIR,R) corresponds to NDVI. In total, there were 45 independent NDSIs computed from the 10 reflectances (Table 2).

Weather data

Daily weather data was downloaded from the SILO spatially-interpolated dataset (Jeffrey et al., 2001), at a 0.1° grid. Comprehensive accuracy metrics for this weather dataset are reported in Jeffrey et al. (2001). For example, cross validation maximum and minimum temperatures across Australia had an RMSE of approximately 1.4 and 1.9 ∘C respectively, although the errors were lower in the study area (southern NSW). For each site, the weather data from the closest location was used. Variables included minimum and maximum temperatures and humidity, evapotranspiration, degree days, solar radiation and rainfall, as shown in Table 2.

Data engineering

The first hypothesis was that rice GMC can be predicted from remote sensing data acquired on the same day (co-incident) as the sample date, as previous work has demonstrated GMC is correlated with NDSIs (Dunn & Dunn, 2021). The second hypothesis was that accumulating weather data from each image date could provide the information needed to forecast GMC beyond the image date. Therefore, the developed models take as inputs all the NDSIs at a given date, and weather variables accumulated on a daily basis from that image date (dI) to each GMC prediction date (dP).

To train the models to forecast GMC using a combination of image and weather data, for each GMC field sample, multiple data rows were created using multiple image dates that preceded the sample date. The time difference between the image date and sample date is referred to as the 'forecast horizon' (dP-dI). This forecast horizon was limited to a maximum of 28 days. When the forecast horizon was 0 days (i.e., the image date equals the sample date), it is called a 'co-incident' prediction, as accumulated weather variables are 0, so it uses only the satellite data. For longer forecast horizons, the model combines the satellite data with accumulated weather variables for the days between the image date and sample/prediction date. This data engineering process is illustrated in Fig. 2, and specified as follows:

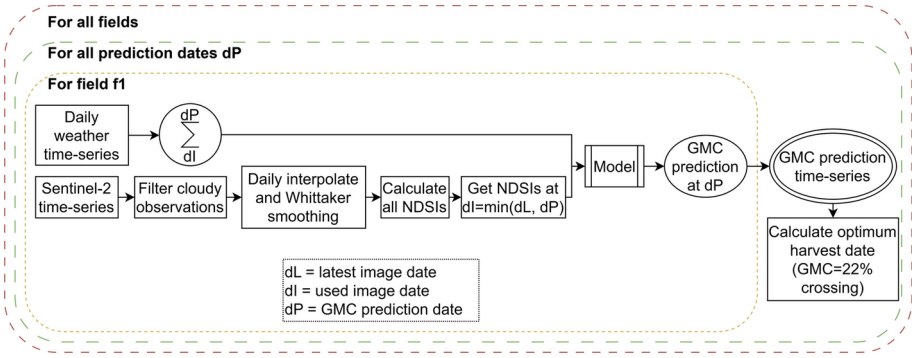

Fig. 2 Diagram of data processing and modeling, showing how image and weather data is integrated to provide grain moisture content (GMC) predictions at each date of interest, and predictions are summarized to determine the optimal harvest date, where NDSIs are the normalized difference spectral indices

```
for each site do
    for each image date do
        for each grain moisture sample date do
            Construct a row with:
                * Site ID
                * Rice variety
                * GMC (%)
                * All NDSIs
                * Weather variables accumulated from image to sample date
        end for
    end for
end for
```

Algorithm 1 Construct data rows

After this process, a dataset with 46,980 rows was obtained, which is 1620 (samples) × 29 (forecast days from 0–28).

In the operational scenario, the system uses the most recent cloud-free image and weather data (observations and forecasts) beyond this to predict future GMC values. This is important to allow a rice grower to plan ahead for field drainage and harvest operations. To model GMC at dates before the latest image date (i.e. where image data co-incident with the desired prediction dates is already available), the accumulated weather variables are zero, so only remote sensing data influences model predictions.

Model training

A range of experiments were performed to assess GMC machine learning (ML) model performance. In experiment 1, the accuracies obtainable using 4 machine learning algorithms (discussed below), and different combinations of remote sensing and accumulated weather features, were compared. In experiment 2, for the best algorithm and combination of features, the performance using TOA and SR remote sensing data was compared. In experiment 3, the selected model accuracy in co-incident (predicting GMC at an available image date)

and forecast (predicting GMC past an image date) scenarios were assessed. These are discussed in more detail in the following.

The three seasons in the dataset varied in terms of phenology progression and weather. Therefore, to robustly evaluate prediction accuracy of various models under variable seasonal scenarios, a leave-one-year-out (LOYO) methodology was used. First, models were trained using [2022,2023] data and tested on [2024] data, then [2022,2024]→[2023], then [2023,2024]→[2022]. This methodology allows robust assessment of errors when applying the models to forecast GMC in a new season that no ground-truth data has been collected for (Filippi et al., 2025).

The results from four algorithms were compared. *Lasso* is a linear regression algorithm that uses L1 regularization, which penalizes the absolute value of the coefficients, resulting in less important coefficients being shrunk to zero. The input features were normalized using their mean and standard deviation from the training data before fitting the model. The regularization hyperparameter "alpha" was optimized as discussed below. *Ridge*, is another linear regression algorithm that uses L2 regularization, which penalizes the square of the coefficients, resulting in less important coefficients being shrunk towards (but not to) zero. The same normalization and hyperparameter optimization as for lasso was performed. *Random forest* (RF) regression is a nonlinear algorithm that ensembles decision trees based on subsamples of the training data and features, and averages their outputs. The hyperparameters that were tuned for RF were the number of estimators and maximum features. *Light gradient boosting machine* (LGB) is an efficient nonlinear algorithm that uses an ensemble of gradient-boosted trees, which are grown leaf-wise (Ke et al., 2017). The tuned hyperparameters for LGB were the number of leaves and minimum child samples. Many functions from the scikit-learn (Pedregosa et al., 2011) libraries were used during this process.

In order to optimize the model hyperparameters mentioned above, a grid search method was employed. The training data was split into four cross validation folds of year $\times$ latitude (above and below $35°$S) in each LOYO experiment. This reduced the chance of the models overfitting either temporally or spatially.

In terms of feature selection, the performance of models using only a single ND (NDVI and also the ND that was found to be most correlated with GMC) were assessed, and compared with models including all 45 NDs. Some of the algorithms are robust in the presence of co-correlated predictors, for example ridge shrinks such predictor's coefficients together (Hastie et al., 2009). In addition, multiple models were trained and assessed using different combinations of weather variables, particularly to assess the relative contributions of temperatures, rainfall and other predictors to GMC dry-down prediction accuracy.

Models were evaluated by how well they predicted the moisture in each of the 3 test years. Metrics evaluated included the root mean squared error (RMSE) of the moisture predictions (%), the R^2 score for regression models (as implemented in scikit-learn) and the average bias between actual and predicted moisture. As a second evaluation step, the time-series of moisture predictions for each site were summarised to find the date where the moisture predictions crossed the optimum harvest moisture (22%), and this predicted date was compared to the actual 22% date obtained by linearly interpolating between the moisture samples on a daily basis to give an error in days.

Generating in-field spatial grain moisture predictions

Since the models were developed using samples taken at point locations, which corresponded to image pixels, it was possible to provide spatial maps of moisture predictions at each Sentinel-2 image date. The accumulated weather coefficients were set to 0 so the model predicted moisture co-incident with the selected image date. The ridge regression model was used, which allows simple porting to GIS systems as a linear equation. The model coefficients were denormalized and an equation relating GMC to the 45 NDSIs was generated and implemented in Google Earth Engine.

Results

Seasonal data

Figure 3a shows all sample data for the three years. The distribution of sample GMCs was similar between the years. There was considerable variation in the average optimal harvest dates (GMC of 22%). The 2023 crops were later on average (mean 9 April), and those in 2024 were earlier (mean 23 March). This can be explained, firstly, by the sowing dates (Fig. 3b). There was great variation in 2023 sowing dates, with many being sown later due

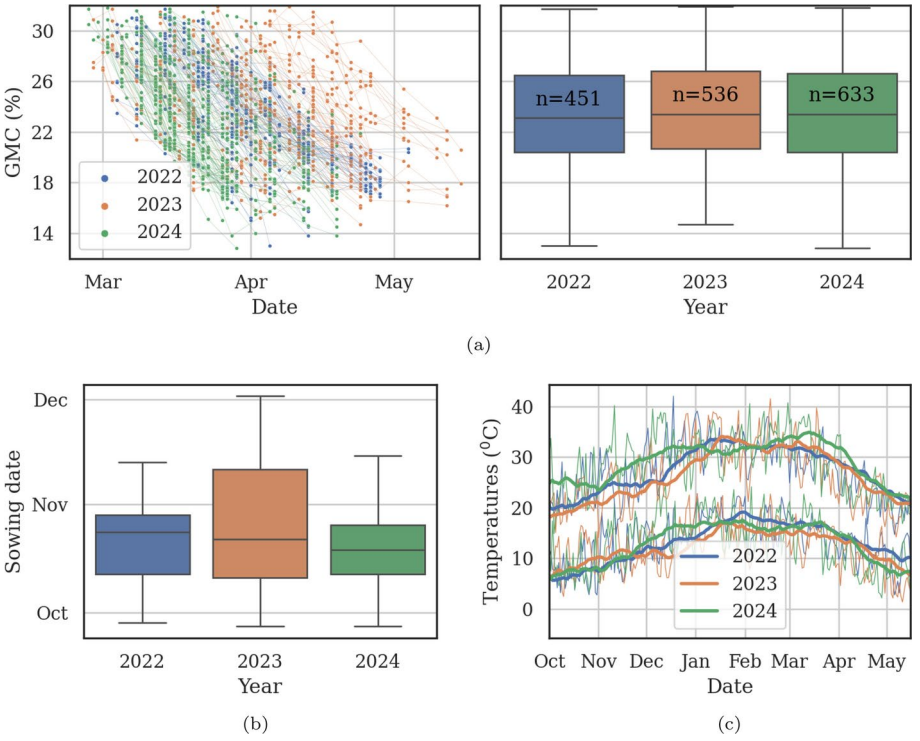

Fig. 3 (**a**) The 1620 rice grain moisture content samples (left, lines show trajectory for each field) and distribution (right) for the 3 years; **(b)** the distribution of sowing dates per year; **c** the minimum and maximum temperatures, daily (thin lines) and 30-day rolling average (thick lines)

to flooding in October-November. Secondly, the weather in 2024 was warmer during both the vegetative stages (December) and during the dry-down period (March-April) (Fig. 3c) than the other years, which accelerated crop progression.

Relationship between grain moisture content and co-incident remote sensing data

Figure 4 shows the average reflectances at each wavelength for samples with GMCs of 21–23% and 27–29%. For higher GMC samples, the reflectances were lower in the B-RE1 bands and in the SWIR1-SWIR2 bands, while the reflectances were higher in the RE2-NIR2 bands. The distinction between the reflectances at different GMCs was consistent between years. These results support the hypothesis that rice GMC may be determined by multispectral imagery of the canopy.

Secondly, the correlation between all 45 NDSIs and GMC was calculated for all samples (Fig. 5a). NDVI=ND(NIR,R) had a Pearson's r of 0.77 and the relationship was somewhat variable between years (Fig. 5b). The strongest correlation was observed for ND(SWIR1,RE3), with r=−0.84, and the relationship was consistent between years (Fig. 5c) and was slightly nonlinear. Generally, the NDSIs that combined shortwave infrared bands with red-edge or near infrared bands (RE2-NIR2) had the highest correlations ($|r| > 0.8$). This can be related to the reflectance profiles (Fig. 4), where for higher GMC the SWIR reflectances are lower and the RE2-NIR2 reflectances are higher, leading to greater differences in the numerator of the respective NDSIs (Eq. 1).

Forecast model example

An example of the data input to a GMC forecast model, with the actual and predicted moisture values, is shown in Fig. 6. The Sentinel-2 observations of ND(SWIR1,RE3) (the NDSI most correlated with GMC) are shown, as well as the smoothed daily data. In this example, that latest clear image was from 10-March. Before this date the accumulated weather variables were 0, while afterwards, the accumulated weather variables take effect. The model can then predict the GMC at each day before and after the latest image date using a combination of these variables. In this example, the model predicted the moisture would cross the optimum harvest moisture of 22% on 22-March, i.e. 12 days forecast past the latest image

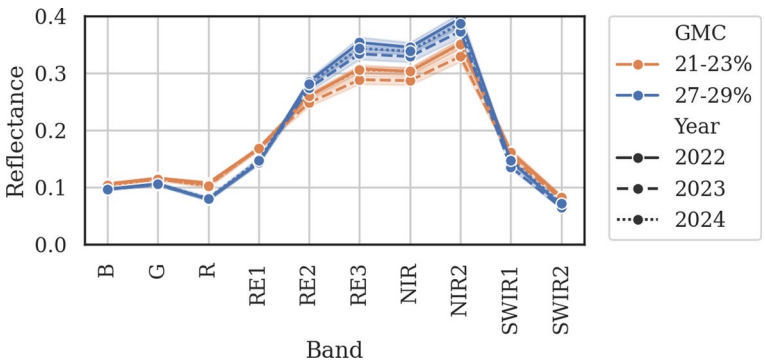

Fig. 4 Reflectance profile of samples at high and low grain moisture content (GMC)

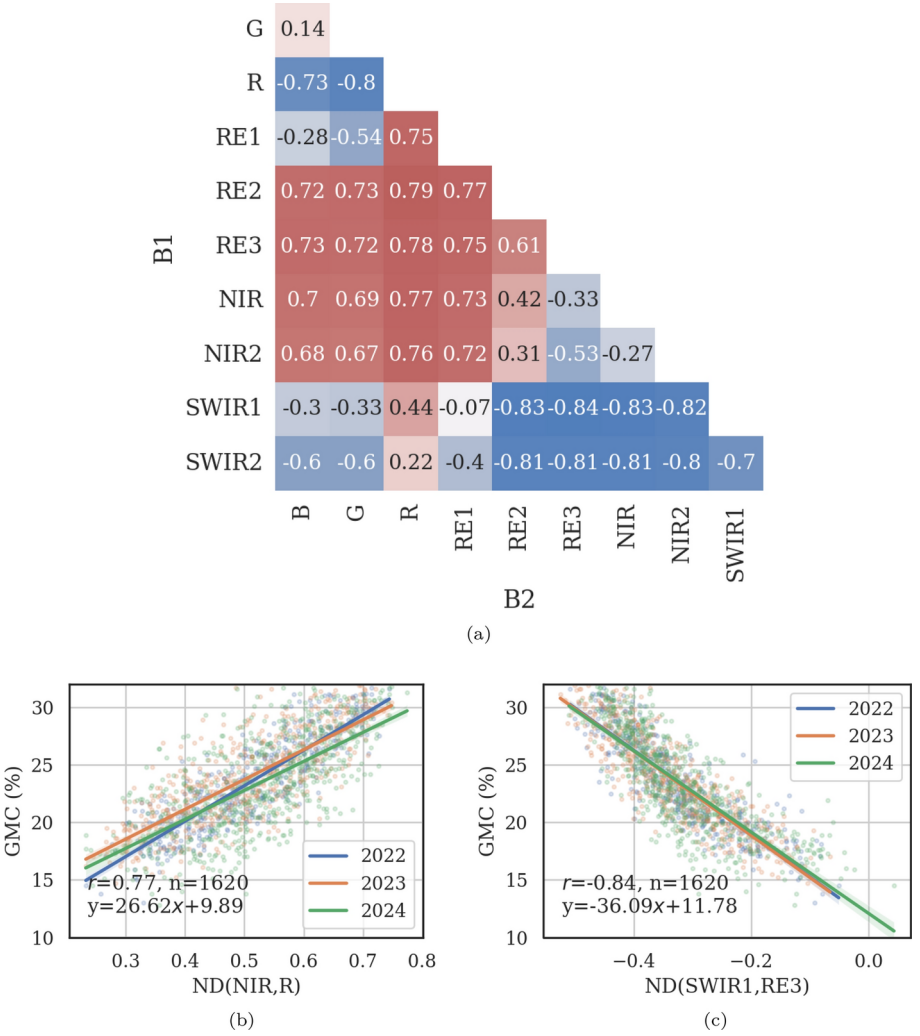

Fig. 5 **a** Correlation coefficient between moisture and normalized difference spectral indices ND(B1,B2); **b** the relationship between NDVI=ND(NIR,R) and grain moisture content (GMC); **c** the relationship between most correlated index ND(SWIR1,RE3) and GMC

date. The actual 22% GMC date (found by linear interpolation of the sample data) was 20-March, giving an error of 2 days.

Forecast model selection

After training models with various combinations of the input variables in Table 2, and assessing predictions on each of the 3 held-out test years in turn, model accuracies in predicting the GMC were calculated, as shown in Fig. 7 (experiment 1). These results were obtained using TOA Sentinel-2 data. Generally, the lowest errors were obtained in 2022, and the highest in 2024.

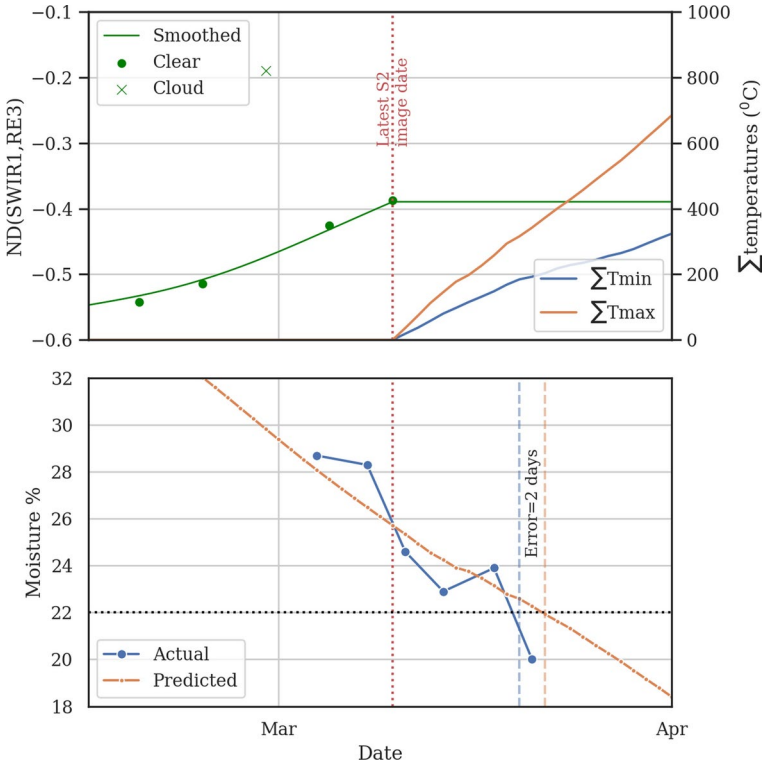

Fig. 6 Example data from one 2024 rice field, showing (top) remote sensing, weather data and (bottom) GMC sample and predictions from the ridge regression model with all normalized difference spectral indices, minimum and maximum temperatures (All ND+Temps)

The best model overall was ridge regression with All ND + Temps variables. For this model, the difference in accuracy using SR instead of TOA data was then investigated (experiment 2). The average of the 3 year RMSEs was 2.09% for TOA, and 2.12% for SR. Therefore, given these insignificant differences in results (with TOA being slightly better), TOA data is used in the following results.

In terms of remote sensing variables, the worst predictions were obtained using NDVI=ND(NIR,R), with ND(SWIR1,RE3) being a much better remote sensing predictor as also noted in the correlation analysis above. However, better results again were obtained when all 45 NDSIs were included, further reducing errors by about 20% (see Fig. 7).

There was no advantage to using all weather predictors (including ET, Srad, RH, DD, Rain, Table 2) compared with just using accumulated temperatures. Using accumulated temperatures proved more effective than accumulated days, for example the ridge models with accumulated days exhibited a 5% higher RMSE compared to those using accumulated temperatures. Adding rain or variety to temperatures did not improve average RMSE for the highest performing algorithms (Lasso, ridge and LGB). Therefore, with the GMC sample dataset in this study, temperatures were sufficient to model dry-down past the most recent remote sensing image. It is possible that larger datasets with more weather variability may be able to exploit relationships between the other weather variables and dry-down.

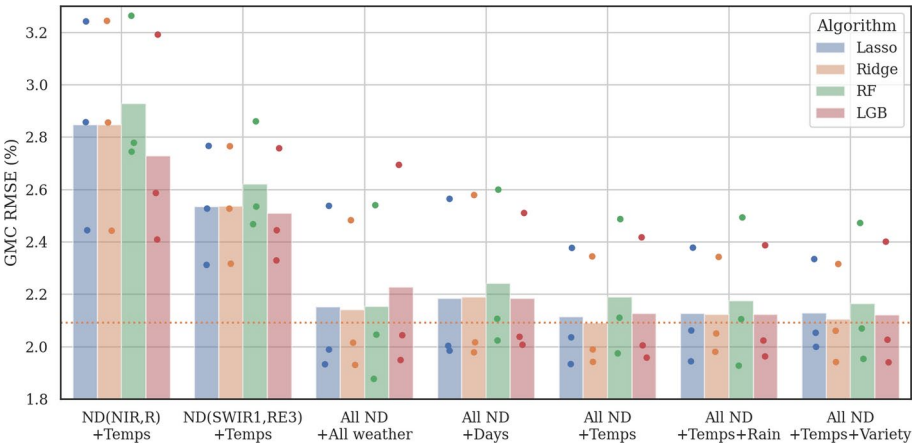

Fig. 7 Comparison of model performance across the 3 test years for a variety of algorithms and feature sets (ND=normalized difference spectral indices, Temps=accumulated minimum and maximum temperatures since the image date, All weather=accumulation of all weather variables, Days=accumulated days, Rain=accumulated rainfall, LGB=Light gradient boosting machine, RF=Random forest); with bar height showing the mean, and the points showing the RMSE for each of the 3 leave-one-year-out test years; and the horizontal orange line showing the best average model performance (ridge with All ND+Temps with RMSE=2.09%)

Of the nonlinear algorithms, LGB usually performed better than random forest, except when all weather variables were included, possibly indicating LGB overfitting to training data in this case. However, the best results overall were obtained with the linear algorithms, with ridge generally giving the lowest errors.

Based on the above results, the models based on the ridge regression algorithm with all NDSIs and accumulated minimum and maximum temperatures (All ND + Temps) were selected for further investigations.

Model accuracy in co-incident and forecast scenarios

Using the selected model parameters discussed above, the GMC predictions as a function of forecast days (i.e. days beyond the end of a truncated remote sensing time-series) were assessed (experiment 3). With 0 forecast days (i.e., predicting moisture on a date where there is remote sensing data available), the RMSE was 2.08%, the bias (average error) was 0% and R^2 was 0.73 (Fig. 8a). The results were slightly worse at 20 days forecast (using accumulated temperatures for 20 days beyond the last remote sensing image), with RMSE increasing by 0.11%, as shown in Fig. 8b. The GMC RMSE for each test year versus forecast days is given in Fig. 8c. Minimum errors were obtained between 5–10 days forecast, indicating the model is optimizing between the extremes of 0 days forecast and 28 days forecast. The highest errors overall were obtained in 2024, whereas 2022 had the lowest minimum errors, but the errors degraded more sharply in 2022 as the forecast horizon was extended.

The actual and predicted date when the moisture dropped below the optimum harvest moisture of 22% was determined for each site, for forecast horizons from 0–28 days (in steps of 4). An example of this process for one 2024 field was shown in Fig. 6, where the

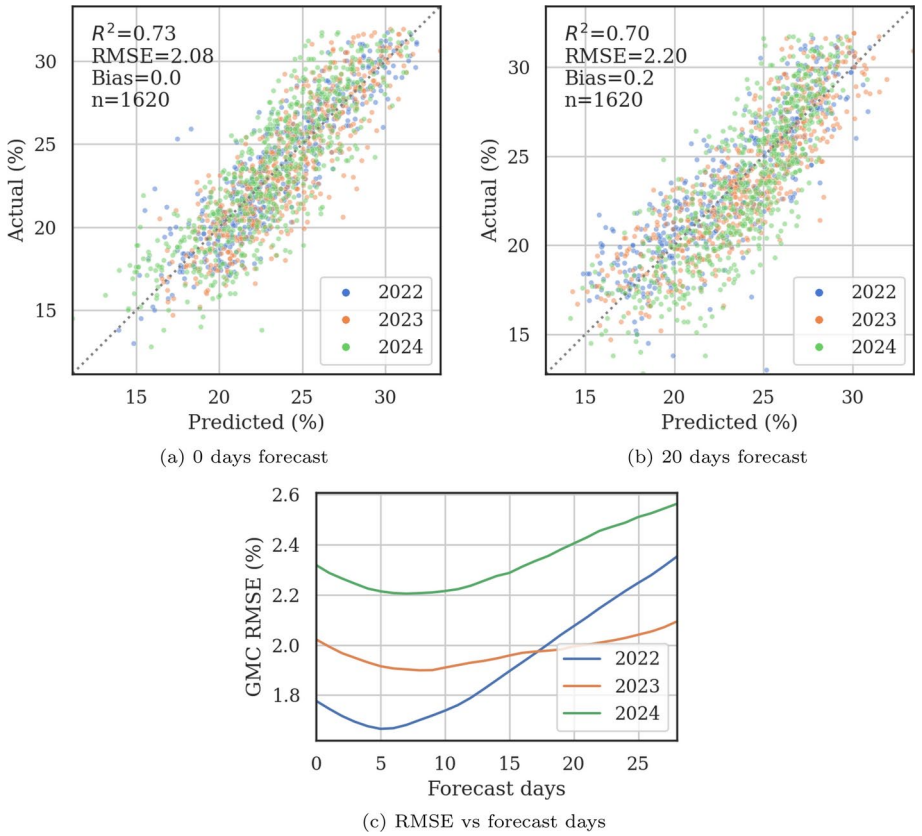

Fig. 8 Grain moisture content (GMC) prediction errors at **a** 0 and **b** 20 days forecast from the respective remote sensing image date, and **c** summary of RMSE for 0–28 forecast days

error at 12 days forecast was 2 days. The actual and predicted dates are compared in Fig. 9. Note that of the 247 sites, 228 had at least one sample with GMC below 22%, so the other 19 sites were excluded from this analysis. The RMSE was 6.6 days for 0 days forecast across the 3 test years, and the bias was 1.7 days (predicted slightly late on average) and R^2 was 0.77 (Fig. 9a). The results at 20 days forecast were similar (Fig. 9b). The reason for the similarity between 0 and 20 days forecast is suggested by Fig. 9c, where the minimum errors are obtained between 8–16 days forecast, with the errors rising for shorter and longer horizons, again indicating the models have optimized for minimum errors across the whole training dataset, which included all forecast horizons from 0–28 days.

In-field spatial predictions

A ridge regression model was trained using 2022–2023 data, and the model was ported to Google Earth Engine as a linear equation. The example in Fig. 10 shows a number of 2024 rice fields, comparing the predicted GMC from the 25-March Sentinel-2 image with samples taken on the same date. For the 6 samples, the moisture content was predicted with R^2=0.7, RMSE=1.95% and bias=0.5%.

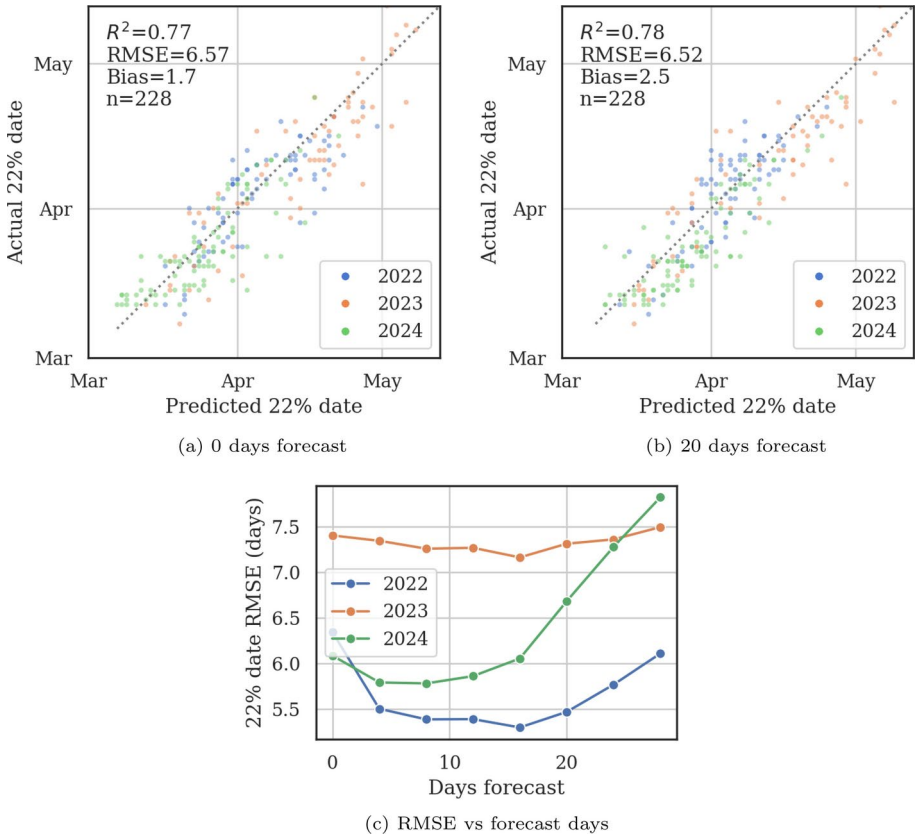

Fig. 9 Grain moisture content (GMC) forecast accuracy at predicting the 22% crossing date, with **a** 0 and **b** 20 days forecast, and **c** summary of RMSE of 22% date predictions for 0–28 forecast days

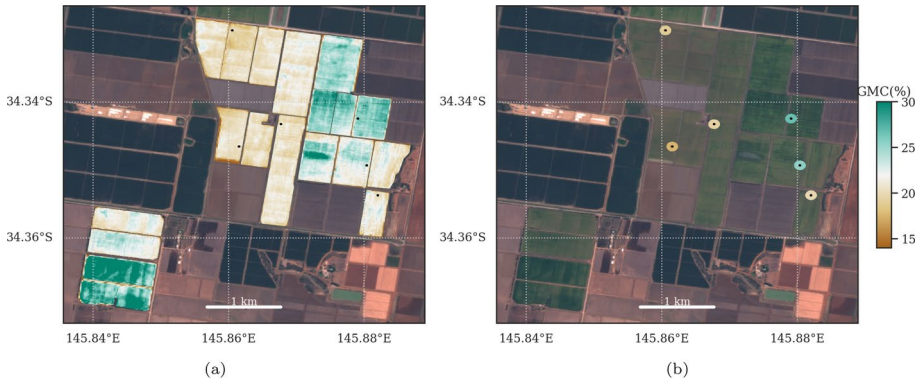

Fig. 10 **a** Grain moisture content (GMC) predictions for fields using 25-March Sentinel-2 image; **b** grain moisture samples taken at point locations in the fields on the same date

Discussion

This study demonstrated firstly that rice GMC has a consistent relationship with normalized difference spectral indices computed from remotely sensed reflectances of the canopy. Secondly, a feature engineering process was developed that enables the forecasting of GMC beyond the latest available remote sensing image date by accumulating weather variables from that date. Investigations of many machine learning algorithms and input variables revealed that ridge regularized linear regression with 45 normalized difference spectral indices and accumulated minimum and maximum temperatures provided optimal predictions. The models could be applied to per-field time-series data to predict optimum harvest date per field, and also deployed in Earth Engine using remote sensing data to provide maps of the spatial variability of GMC.

Remote sensing data and indices

In line with other recent research, this work has shown that indices derived from optical remote sensing data are effective predictors of GMC. For example, Brinkhoff et al. (2023) found that rice nitrogen status affected time from flowering to harvest readiness, suggesting that remote sensing may have potential to parameterize such impacts. Peng et al. (2024) found that the difference between absorption coefficients in the blue and red bands was correlated with rice panicle dry biomass, with $R^2 = 0.81$, which they attributed to relative changes in chlorophyll and carotenoid absorption during senescence. Dunn and Dunn (2021) found that rice GMC was correlated with NDVI, though the relationship varied with variety. Similarly. the current work showed that the relationship between NDVI and GMC also varied with season. However, the relationship with another spectral index based on a shortwave infrared (SWIR1 at 1610nm) and red edge band (RE3 at 780nm) had higher correlation and the relationship was consistent between seasons. The wavelength of the red edge band was important, as the correlation was very low when using a shorter wavelength Sentinel-2 band (RE1 at 705nm), because as Fig. 4 indicated, the rise in reflectance in SWIR1 and RE1 bands with decreasing GMC is similar, whereas the change is opposite and thus magnified for SWIR1 and RE3.

However, even when using this optimal NDSI ND(SWIR1,RE3) in models, the independent test results had a relatively high RMSE around 2.5% (Fig. 7). Model performance was greatly improved when all 45 independent NDSIs were used, with RMSE reducing to around 2.1%. Utilizing this large number of features relied on the machine learning algorithms limiting model complexity with hyperparameters optimized using leave-one-year-region-out cross validation.

While many works assume that surface reflectance (SR) remote sensing data will provide superior predictions to top of atmosphere (TOA) data, this research explicitly examined models trained and tested using Sentinel-2 TOA (L1C) and SR (L2A) data. The results were similar, with TOA even being slightly better (2.09 vs 2.12% RMSE). Though this may be considered counter-intuitive, other works have likewise found little if any benefit of using SR instead of TOA data when coupled with ML models (Wolters et al., 2021; Brinkhoff et al., 2022). This may possibly be due in part to errors in atmospheric correction processes, and models learning to correct for variances in atmospheric effects if sufficient data and features are supplied to the model (Medina-Lopez, 2020). The use of TOA

data brings further benefits of requiring less processing compute and time (Estévez et al., 2022), and consistency across datasets stored in different repositories, so a model trained using data from one repository can be applied to data stored from a different repository if needed (whereas the atmospheric correction used to generate SR products may be inconsistent between repositories).

Weather data for forecasting beyond the latest remote sensing image

The weather data used in this study was from the SILO dataset, which processes observation data to a daily time step and spatially interpolates between weather stations (Jeffrey et al., 2001). We acquired this data at a $0.1°$ grid, approximately 10km. As the terrain in the study area is relatively flat, there is unlikely to be significant variation in conditions at this scale. However, water bodies, such as those in rice fields, may cause local variation in some weather parameters. Incorporating these effects to adjust weather forecasts would be challenging, but may provide some accuracy improvements.

The developed methodology of using weather variables accumulated on a daily basis past the latest remote sensing image to forecast GMC was successful to extend the prediction horizon. The models had a u-shaped error profile from 0 to 28 days forecast, indicating the models optimized for errors in the middle of the forecast range. Models trained using accumulated temperatures had around 5% lower RMSE compared to simply accumulating days, indicating the models were able to learn the impact of weather conditions on the rate of rice GMC dry-down. In contrast, some studies did not find conclusive advantage of including weather in dry-down model parameters (Martinez-Feria et al., 2019; Brinkhoff et al., 2023). In order for models to learn predictive features from weather data, a significant degree of weather variability in the training dataset is needed. The current study included a cold (2023) and a hot (2024) year. Similarly (Chazarreta et al., 2023) used a dataset with a wider range of sowing dates, and hence variability in weather conditions during various stages of crop phenology, finding that including weather variables in the dry-down coefficient did offer benefit. The models developed in this work could be improved by utilizing additional seasons of data with a wider range of weather conditions, which also may potentially demonstrate that incorporating weather variables beyond temperature enhances prediction accuracy.

Operational implementation

The developed methodology has been incorporated into an operational near-real-time rice monitoring system. Each grower can access per-field information, including phenology, nitrogen, growth trajectories and the GMC forecasts this work focused on. These GMC forecasts facilitate improved advance planning of the timing of field drainage and harvest for each field.

To do this, the system processes Sentinel-2 remote sensing data for each field as soon as it is available. Then weather observations and forecasts are combined to provide the most accurate expectation of conditions at each date (Brinkhoff et al., 2023). Weather forecasts to 16 days are obtained from the Global Forecast System data, produced by the National Centers for Environmental Prediction, and which are available in Earth Engine. This provides the required weather variables at a 3-hour interval that are summarized to a daily basis (e.g.

daily minimum and maximum temperatures and total rainfall), to produce variables that align with the SILO observation data. To forecast grain moisture beyond 16 days, the average of observations from the SILO dataset at each date and location since 2000 is used. As model predictions are dependent on weather forecast accuracy, they are thus more accurate at shorter forecast horizons. GMC forecasts are updated using the latest remote sensing and weather data on a daily basis.

This is expected to reduce farmer resources devoted to visiting many fields spread over large distances to gather field samples. It also has the advantage of using data from across entire fields, as it is based on spatially distributed remote sensing data, rather than point sample locations, which may misrepresent the GMC status of the field as a whole.

Further research

The developed models were able to predict the date a field will reach a given moisture level, for example the optimum harvest moisture of 22%. This can help support decisions leading to improved grain quality. One topic that needs further research is to use these models to also optimize field drainage dates. This is more complicated, as many factors impact on the drainage date decision. These factors include the importance of reaching physiological maturity before imposing any water stress to ensure yield potential is reached (Counce et al., 1990) and to minimize chance of stem weakening and lodging (Dunn & Dunn, 2023), the impact of field layout and surface conditions on time for water to drain (North et al., 2010), evapotranspiration variability affecting how quickly residual water and soil moisture is used (Linquist et al., 2015), and the need to ensure fields are dry enough to enable trafficability by mechanized harvesters.

While the models were able to predict optimum harvest date with reasonable accuracy (RMSE around 6.5 days and R^2 above 0.75 and bias less than 3 days), further research should aim to reduce these errors further. The samples in this study were not distributed evenly among rice varieties, but rather reflected the proportions of each variety currently grown in the study area. This may be the reason the models were not improved by adding variety as a model variable. Further work should include evaluation of the impact of variety on models, which may reduce errors for varieties that aren't as strongly represented in training data. Additionally, including other variables in the predictor sets may further improve the models, such as flowering date, soil type and field drainage parameters (e.g. slope and roughness).

The models in this paper were calibrated using field samples taken from point locations. Several sources of error in this process could contribute to reduced precision from model predictions. Firstly, while sampling locations targeted areas with relatively uniform crop vigor, there was significant variability in grain moisture across many fields (Fig. 10a). The Sentinel-2 pixels are at 10 or 20 meters depending on band, so that point samples may not always accurately describe the mean of the moisture content within a whole pixel. Additional errors may be introduced by the grain moisture content measurements. To mitigate these effects, this study used a very large number of samples taken across many fields and from multiple seasons, reducing the impact of errors of individual samples.

The results demonstrated that remotely sensed reflectances have a strong relationship with rice grain moisture content. The samples included diverse seasons, management strategies, varieties and biomass. However, when scaling up to cover all pixels within many

fields across entire growing regions, it is possible that factors such as pest damage, disease and weeds may influence retrieved reflectances and thus reduce the accuracy of grain moisture content predictions. If such cases are relatively common, it may be necessary to develop a preliminary step that excludes unrepresentative or non-rice pixels from within field boundaries.

This work considered multi-spectral data. Data from thermal infrared and synthetic aperture radar sensors could also be exploited to improve GMC prediction models, as these contain information related to the water status of surfaces (Steele-Dunne et al., 2017; Khanal et al., 2017). This point will become increasingly pertinent as higher spatial and temporal resolution data from thermal and radar sensors is made available.

Conclusion

A methodology was developed to enable the prediction of rice grain moisture content (i) from co-incident remote sensing imagery and (ii) beyond the latest available image by using accumulated weather forecast data. For the three years and 247 sites, the average moisture prediction error (RMSE) was 2.1% and the average prediction of the optimum harvest date (22% moisture) had an RMSE around 6.5 days. The models can be operationalized in rice monitoring systems to provide daily updated predictions, which will provide benefits to rice farmers in supporting decision-making regarding optimal field drainage and harvest timing with the aim of reaching the highest possible yield and quality.

Acknowledgements This work was funded by AgriFutures Australia, grant PRO-013078 (Real-time remote-sensing based monitoring for the rice industry). Samples were gathered and processed by staff at the New South Wales Department of Primary Industries and Regional Development and Sunil Jha. We are grateful for helpful discussions and practical suggestions from the Rice Extension team, including Mark Groat, Peter McDonnell, Chris Quirk and Anna Jewell. We appreciate the suggestions the reviewers and editor of this paper provided, which resulted in an improved manuscript.

Funding Open Access funding enabled and organized by CAUL and its Member Institutions

Data availability Data presented in this study is confidential.

Declarations

Conflicts of Interest The authors declare that they have no conflict of interest.

References

AACC (1999). *AACC International Method 44-15.02. Moisture–Air-Oven Methods. Reapproval November 3, 1999.* Retrieved 2024-12-20, from http://dx.doi.org/10.1094/AACCIntMethod-44-15.02

Abdollahpour, S., Kosari-Moghaddam, A., & Bannayan, M. (2020). Prediction of wheat moisture content at harvest time through ANN and SVR modeling techniques. *Information Processing in Agriculture,7*(4), 500–510. https://doi.org/10.1016/j.inpa.2020.01.003

Brinkhoff, J., Clarke, A., Dunn, B. W., & Groat, M. (2024). Analysis and forecasting of Australian rice yield using phenology-based aggregation of satellite and weather data. *Agricultural and Forest Meteorology,353*, 110055. https://doi.org/10.1016/j.agrformet.2024.110055

Brinkhoff, J., Dunn, B. W., & Dunn, T. (2023). The influence of nitrogen and variety on rice grain moisture content dry-down. *Field Crops Research,302*, 109044. https://doi.org/10.1016/j.fcr.2023.109044

Brinkhoff, J., Houborg, R., & Dunn, B. W. (2022). Rice ponding date detection in Australia using Sentinel-2 and Planet Fusion imagery. *Agricultural Water Management,273*, 107907. https://doi.org/10.1016/j.agwat.2022.107907

Brinkhoff, J., McGavin, S. L., Dunn, T., & Dunn, B. W. (2023). Predicting rice phenology and optimal sowing dates in temperate regions using machine learning. *Agronomy Journal,116*(3), 871–885. https://doi.org/10.1002/agj2.21398

Calderwood, D. L., Bollich, C. N., & Scott, J. E. (1980). Field Drying of Rough Rice: Effect on Grain Yield, Milling Quality, and Energy Saved. *Agronomy Journal,72*(4), 649–653. https://doi.org/10.2134/agronj1980.00021962007200040019x

Chazarreta, Y. D., Carcedo, A. J. P., Alvarez Prado, S., Massigoge, I., Amas, J. I., Fernandez, J. A., & Otegui, M. E. (2023). Enhancing maize grain dry-down predictive models. *Agricultural and Forest Meteorology,334*, 109427. https://doi.org/10.1016/j.agrformet.2023.109427

Clarke, A., Yates, D., Blanchard, C., Islam, M. Z., Ford, R., Rehman, S., & Walsh, R. (2024). The effect of dataset construction and data pre-processing on the eXtreme Gradient Boosting algorithm applied to head rice yield prediction in Australia. *Computers and Electronics in Agriculture,219*, 108716. https://doi.org/10.1016/j.compag.2024.108716

Counce, P. A., Siebenmorgen, T. J., Vories, E. D., & Pitts, D. J. (1990). Time of Draining and Harvest Effects on Rice Grain Yield and Quality. *Journal of Production Agriculture,3*(4), 436–445. https://doi.org/10.2134/jpa1990.0436

Dingkuhn, M., & Le Gal, P.-Y. (1996). Effect of drainage date on yield and dry matter partitioning in irrigated rice. *Field Crops Research,46*(1), 117–126. https://doi.org/10.1016/0378-4290(95)00094-1

Dunn, B., & Dunn, T. (2021). *Predicting rice crop maturity using remote sensing* (Tech. Rep.). NSW Deparment of Primary Industries. Retrieved 2024-12-20, https://www.dpi.nsw.gov.au/__data/assets/pdf_file/0009/1365192/SRR21-book-web-cm29Oct2021.pdf

Dunn, B. W., Dunn, T. S., & Beecher, H. G. (2014). Nitrogen timing and rate effects on growth and grain yield of delayed permanent-water rice in south-eastern Australia. *Crop and Pasture Science,65*(9), 878–887. https://doi.org/10.1071/CP13412

Dunn, B. W., & Gaydon, D. S. (2011). Rice growth, yield and water productivity responses to irrigation scheduling prior to the delayed application of continuous flooding in south-east Australia. *Agricultural Water Management,98*(12), 1799–1807. https://doi.org/10.1016/j.agwat.2011.07.004

Dunn, T., & Dunn, B. (2023). *Lodging in rice* (DPI Primefact). Retrieved 2024-08-20, from https://www.dpi.nsw.gov.au/__data/assets/pdf_file/0008/719855/Lodging-in-rice.pdf

Eilers, P. H. C. (2003). *A Perfect Smoother. Analytical Chemistry,75*(14), 3631–3636. https://doi.org/10.1021/ac034173t

Estévez, J., Salinero-Delgado, M., Berger, K., Pipia, L., Rivera-Caicedo, J. P., Wocher, M., & Verrelst, J. (2022). Gaussian processes retrieval of crop traits in Google Earth Engine based on Sentinel-2 top-of-atmosphere data. *Remote Sensing of Environment,273*, 112958. https://doi.org/10.1016/j.rse.2022.112958

Filippi, P., Han, S. Y., & Bishop, T. F. (2025). On crop yield modelling, predicting, and forecasting and addressing the common issues in published studies. *Precision Agriculture,26*(1), 8. https://doi.org/10.1007/s11119-024-10212-2

Flor, O., Palacios, H., Suárez, F., Salazar, K., Reyes, L., González, M., & Jiménez, K. (2022). New Sensing Technologies for Grain Moisture. *Agriculture,12*(3), 386. https://doi.org/10.3390/agriculture12030386

Gorelick, N., Hancher, M., Dixon, M., Ilyushchenko, S., Thau, D., & Moore, R. (2017). Google Earth Engine: Planetary-scale geospatial analysis for everyone. *Remote Sensing of Environment,202*, 18–27. https://doi.org/10.1016/j.rse.2017.06.031

Hastie, T., Tibshirani, R., & Friedman, J. (2009). *The Elements of Statistical Learning*. New York, NY: Springer, New York.

Humphreys, E., Lewin, L. G., Khan, S., Beecher, H. G., Lacy, J. M., Thompson, J. A., & Dunn, B. W. (2006). Integration of approaches to increasing water use efficiency in rice-based systems in southeast Australia. *Field Crops Research,97*(1), 19–33. https://doi.org/10.1016/j.fcr.2005.08.020

Jeffrey, S. J., Carter, J. O., Moodie, K. B., & Beswick, A. R. (2001). Using spatial interpolation to construct a comprehensive archive of Australian climate data. *Environmental Modelling & Software,16*(4), 309–330. https://doi.org/10.1016/S1364-8152(01)00008-1

Ke, G., Meng, Q., Finley, T., Wang, T., Chen, W., Ma, W., & Liu, T.-Y. (2017). LightGBM: A Highly Efficient Gradient Boosting Decision Tree. *Advances in Neural Information Processing Systems* (Vol. 30). Curran Associates, Inc. Retrieved 2022-08-04, from https://proceedings.neurips.cc/paper/2017/hash/6449f44a102fde848669bdd9eb6b76fa-Abstract.html

Khanal, S., Fulton, J., & Shearer, S. (2017). An overview of current and potential applications of thermal remote sensing in precision agriculture. *Computers and Electronics in Agriculture,139*, 22–32. https://doi.org/10.1016/j.compag.2017.05.001

Linquist, B., Snyder, R., Anderson, F., Espino, L., Inglese, G., Marras, S., & Hill, J. (2015). Water balances and evapotranspiration in water- and dry-seeded rice systems. *Irrigation Science,33*(5), 375–385. https://doi.org/10.1007/s00271-015-0474-4

Martinez-Feria, R. A., Licht, M. A., Ordóñez, R. A., Hatfield, J. L., Coulter, J. A., & Archontoulis, S. V. (2019). Evaluating maize and soybean grain dry-down in the field with predictive algorithms and genotype-by-environment analysis. *Scientific Reports,9*(1), 7167. https://doi.org/10.1038/s41598-019-43653-1

McCauley, G. N., & Way, M. O. (2002). Drain and harvest timing affects on rice grain drying and whole-milled grain. *Field Crops Research,74*(2), 163–172. https://doi.org/10.1016/S0378-4290(01)00205-2

Medina-Lopez, E. (2020). Machine Learning and the End of Atmospheric Corrections: A Comparison between High-Resolution Sea Surface Salinity in Coastal Areas from Top and Bottom of Atmosphere Sentinel-2 Imagery. *Remote Sensing,12*(18), 2924. https://doi.org/10.3390/rs12182924

North, S., Griffin, D., Grabham, M., & Gillies, M. (2010). Improving the performance of basin irrigation layouts in the southern Murray-Darling Basin. *CRC for Irrigation Futures technical report 09/10*,, Retrieved 2024-12-20, from https://www.researchgate.net/publication/265041067

Nowak, B. (2021). Precision Agriculture: Where do We Stand? A Review of the Adoption of Precision Agriculture Technologies on Field Crops Farms in Developed Countries. *Agricultural Research,10*(4), 515–522. https://doi.org/10.1007/s40003-021-00539-x

Pasquarella, V.J., Brown, C.F., Czerwinski, W., & Rucklidge, W.J. (2023). Comprehensive quality assessment of optical satellite imagery using weakly supervised video learning. *2023 IEEE/CVF Conference on Computer Vision and Pattern Recognition Workshops (CVPRW)* (pp. 2125–2135).

Pedregosa, F., Varoquaux, G., Gramfort, A., Michel, V., Thirion, B., Grisel, O., & Duchesnay, E. (2011). Scikit-learn: Machine Learning in Python. *Journal of Machine Learning Research*, *12*(Oct), 2825–2830, Retrieved 2019-04-08, from http://www.jmlr.org/papers/v12/pedregosa11a.html

Peng, S., & Cassman, K. G. (1998). Upper Threshholds of Nitrogen Uptake Rates and Associated Nitrogen Fertilizer Efficiencies in Irrigated Rice. *Agronomy Journal,90*(2), 178–185. https://doi.org/10.2134/agronj1998.00021962009000020010x

Peng, Y., Solovchenko, A., Zhang, C., Shurygin, B., Liu, X., Wu, X., & Gitelson, A. (2024). Remote sensing of rice phenology and physiology via absorption coefficient derived from unmanned aerial vehicle imaging. *Precision Agriculture,25*(1), 285–302. https://doi.org/10.1007/s11119-023-10068-y

R. Lu, T. J. Siebenmorgen, T. A. Costello, E. O. Fryar Jr. (1995). Effect of Rice Moisture Content at Harvest on Economic Return. *Applied Engineering in Agriculture*, *11*(5), 685–690, https://doi.org/10.13031/2013.25792

Schmid, M., Rath, D., & Diebold, U. (2022). Why and How Savitzky-Golay Filters Should Be Replaced. *ACS Measurement Science Au,2*(2), 185–196. https://doi.org/10.1021/acsmeasuresciau.1c00054

Sharifi, H., Hijmans, R. J., Hill, J. E., & Linquist, B. A. (2018). Water and air temperature impacts on rice (Oryza sativa) phenology. *Paddy and Water Environment,16*(3), 467–476. https://doi.org/10.1007/s10333-018-0640-4

Siebenmorgen, T.J., R. C. Bautista, P. A. Counce. (2007). Optimal Harvest Moisture Contents for Maximizing Milling Quality of Long- and Medium-Grain Rice Cultivars. *Applied Engineering in Agriculture*, *23*(4), 517–527, https://doi.org/10.13031/2013.23476

Steele-Dunne, S. C., McNairn, H., Monsivais-Huertero, A., Judge, J., Liu, P.-W., & Papathanassiou, K. (2017). Radar Remote Sensing of Agricultural Canopies: A Review. *IEEE Journal of Selected Topics in Applied Earth Observations and Remote Sensing,10*(5), 2249–2273. https://doi.org/10.1109/JSTARS.2016.2639043

Wang, J., Sun, X., Xu, Y., Wang, Q., Tang, H., & Zhou, W. (2021). The effect of harvest date on yield loss of long and short-grain rice cultivars (Oryza sativa L.) in Northeast China. *European Journal of Agronomy*, *131*, 126382, https://doi.org/10.1016/j.eja.2021.126382

Ward, R., Brickhill, H., Bull, N., Dunn, B., Dunn, T., Fowler, J., & Mauger, T. (2021). Rice Growing Guide 2021. (Vol. 2nd edition). NSW Department of Primary Industries. Retrieved 2024-12-20, from https://www.dpi.nsw.gov.au/__data/assets/pdf_file/0004/1361173/RGG-2021-web-final-26Oct2021.pdf

Wolters, S., Söderström, M., Piikki, K., Reese, H., & Stenberg, M. (2021). Upscaling proximal sensor N-uptake predictions in winter wheat (Triticum aestivum L.) with Sentinel-2 satellite data for use in a decision support system. *Precision Agriculture*, *22*(4), 1263–1283, https://doi.org/10.1007/s11119-020-09783-7

Wu, Z., Luo, J., Rao, K., Lin, H., & Song, X. (2024). Estimation of wheat kernel moisture content based on hyperspectral reflectance and satellite multispectral imagery. *International Journal of Applied Earth Observation and Geoinformation,126*, 103597. https://doi.org/10.1016/j.jag.2023.103597

Xu, J., Meng, J., & Quackenbush, L. J. (2019). Use of remote sensing to predict the optimal harvest date of corn. *Field Crops Research,236*, 1–13. https://doi.org/10.1016/j.fcr.2019.03.003

Yang, M.-D., Hsu, Y.-C., Tseng, W.-C., Lu, C.-Y., Yang, C.-Y., Lai, M.-H., & Wu, D.-H. (2021). Assessment of Grain Harvest Moisture Content Using Machine Learning on Smartphone Images for Optimal Harvest Timing. *Sensors,21*(17), 5875. https://doi.org/10.3390/s21175875

Yang, M.-D., Hsu, Y.-C., Tseng, W.-C., Tseng, H.-H., & Lai, M.-H. (2025). Precision assessment of rice grain moisture content using UAV multispectral imagery and machine learning. *Computers and Electronics in Agriculture,230*, 109813. https://doi.org/10.1016/j.compag.2024.109813